Unmanned Systems, Vol. 10, No. 1 (2022) 93–108

DOI: 10.1142/S2301385022500054

UNMANNED SYSTEMS
https://www.worldscientific.com/worldscinet/us

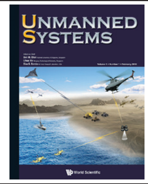

Optimal Autonomous Pursuit of an Intruder on a Grid Aided by Local Node and Edge Sensors

Sufal Chandra Swar[*,¶], Suresh Manickam[*], David Casbeer[†],
Krishna Kalyanam[‡], Swaroop Darbha[§]

[*]*Aeronautical Development Establishment (ADE)*
Defence Research and Development Organization (DRDO)
New Thippasandra Post, Bengaluru 560075, India

[†]*Control Science Center of Excellence*
Air Force Research Laboratory (AFRL)
Wright-Patterson Air Force Base, OH 45433, USA

[‡]*Aviation Systems Division*
NASA Ames Research Center
Moffett Field, CA 94035, USA

[§]*Mechanical Engineering Department*
Texas A & M University (TAMU)
College Station, TX 77843, USA

Timely detection of intruders ensures the safety and security of high valued assets within a protected area. This problem takes on particular significance across international borders and becomes challenging when the terrain is porous, rugged and treacherous in nature. Keeping an effective vigil against intruders on large tracts of land is a tedious task; currently, it is primarily performed by security personnel with automatic detection systems in passive supporting roles. This paper discusses an alternate autonomous approach by utilizing one or more Unmanned Vehicles (UVs), aided by smart sensors on the ground, to detect and localize an intruder. To facilitate autonomous UV operations, the region is equipped with Unattended Ground Sensors (UGSs) and laser fencing. Together, these sensors provide time-stamped location information (node and edge detection) of the intruder to a UV. For security reasons, we assume that the sensors are not networked (a central node can be disabled bringing the whole system down) and so, the UVs must visit the vicinity of the sensors to gather the information therein. This makes the problem challenging in that pursuit must be done with local and likely delayed information. We discretize time and space by considering a 2D grid for the area and unit speed for the UV, i.e. it takes one time unit to travel from one node to an adjacent node. The intruder is slower and takes two time steps to complete the same move. We compute the min–max optimal, i.e. minimum number of steps to capture the intruder under worst-case intruder actions, for different number of rows and columns in the grid and for both one and two pursuers.

Keywords: UV; intruder detection; localization; smart sensors.

1. Introduction

The first layer of defense in ensuring border safety and security is to detect, localize and engage intruders even before an intrusion has taken full effect [1]. Keeping an effective vigil against intruders on vast tracts of interest under all weather conditions is an arduous task; presently, the task of intruder detection, localization and engagement is being executed primarily by personnel with automatic detection systems in supporting roles. The current practice is expensive, fallible and can result in a loss of life. To overcome the deficiencies in current practice, we propose to

Received 12 April 2019; Revised 28 May 2021; Accepted 28 May 2021; Published 10 July 2021. This paper was recommended for publication in its revised form by editorial board member, Yunfeng Zhang.
Email Address: ¶*sufal@ade.drdo.in*

January 5, 2022 1:47:27pm WSPC/284-US 2250005 ISSN: 2301-3850 2nd Reading

employ multiple Unmanned Vehicles (UVs) to detect and localize intruders with the aid of Unattended Ground Sensors (UGSs) and Laser Fence Systems (LFSs) [2]. UGS and LFS store time-stamped information about the passing intruder and provide this information to a UV upon querying. In particular, the UGS provides node detection and tells the UV if and when an intruder occupied that node. The LFS on the other hand, provides edge detection and tells the UV if and when an intruder crossed the concerned edge (and in which direction). Suppose a UV arrives at a triggered node (UGS therein has recorded an intruder passing through). Based on this information, a UV can compute the time that has elapsed since the intruder left the UV's current location; we refer to this elapsed time as information delay.

Intruders crossing a boundary typically move along a network of pathways and are methodical and slow; their actions are typically not random and are intended to serve a specific purpose, e.g. to reach a location within the protected area. In this regard, it makes sense to place motion constraints on the intruder and constrain it to a known set of actions (we assume here that the pursuit team is aware of this set). The objective here is to establish an optimal pursuit policy for the UVs, which guarantees the capture of the intruder with the aid of UGS and LFS, irrespective of actions taken by the intruder from the pre-specified action set. Based on the information received from UGS and LFS, the UVs face the following decision problem: what sequence of actions should the UVs take to localize (capture) the intruder in minimum time? Since we discretize both time and space, this problem is naturally posed as a min–max pursuit on a graph.

A related autonomous border surveillance application where unmanned assets are used to patrol target areas is presented in [3]. Efficient allocation of sensors to track targets in a complex mobile surveillance network is discussed in [4]. A Genetic Algorithm-based system for tasking a team of Unmanned Aerial Vehicles (UAVs) to complete a coordinated surveillance mission is presented in [5,6].

Closely related min–max decision problems were considered in [7–12]; min-max decision problems in graph search using the framework of pursuit evasion games is discussed in [13]. Krishnamoorthy *et al.* [14] present a sufficient condition for guaranteed capture for various information lag in a 2D graph. In [15], the authors provide a min–max optimal pursuit policy for a single UAV on a network with exactly three corridors (or rows) on which the intruder can travel (from left to right). In [16], the authors extend this result to two UAVs operating on an infinite 2D grid. Related research on pursuit on a graph have been reported in [17,18]. This paper is a generalization of the work reported in [15,16] and differs from these in the addition of LFS; the UGS will be used in an identical manner. Specifically, LFS provide more information (edge detection) and consequently guarantees faster capture than with UGSs alone. The pursuit policy in [15,16] is based on the current location of the UAV along with the history of control actions it has taken since the last time it was present at a location visited by the intruder. In this paper, we present a pursuit policy in a similar spirit, but with the presence of additional information from LFS. We also present cooperative pursuit policy for multiple UVs to accomplish intruder detection and localization.

2. Problem Motivation and Contribution

This paper is motivated by the cross border scenario depicted in Fig. 1, where the terrain may be porous, rugged and treacherous in nature. A long border separates two regions I and II as shown in the figure. Each region is equipped with a monitoring tower as well as guarding and patrol personnel. The intruders from region II enter region I with the intention of damaging the resources in region I. In order to detect the intruders' movements automatically, the border is equipped with static autonomous detection systems. Figure 2 shows the expanded view of one section of

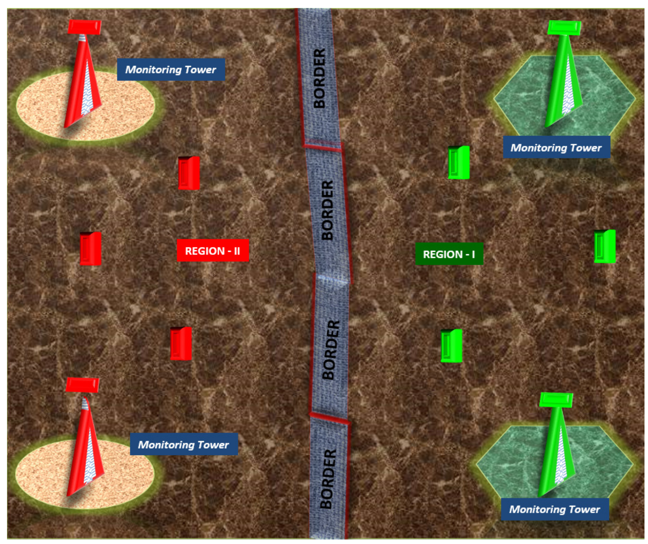

Fig. 1. Cross border mission scenario.

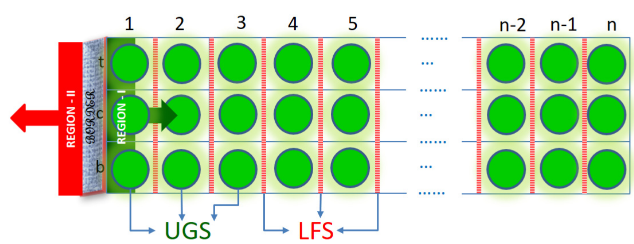

Fig. 2. Cross border mission scenario with UGS and LFS (expanded view).

near-border zone. It can be seen that, the zone in region I is divided into many cells and each cell is equipped with UGS; such a decomposition (assumption) allows us to pose the problem as pursuit-evasion on a graph. Every UGS is capable of detecting objects passing over it and keeps a log of the time-stamped intrusion information.

As mentioned earlier, when a UV queries a UGS in its proximity, it transmits the information log to the UV.

In addition, the *columnar* edges of the cell are equipped with LFS units, which are capable of detecting and identifying any moving object. Each unit stores this information of intruder's movement towards *east* and is linked to adjacent preceding UGS. When a UV is within communication radius of this UGS, it receives the information on direction of move of intruder because of LFS, whenever applicable, in addition to time-stamped intrusion information from the nearby UGS.

The problem at hand may be mathematically formulated as follows: Given (i) a terrain and grid network with each cell equipped with UGS and some edges equipped with LFS and (ii) intruder's movements restricted to a pre-determined action set, determine an optimal pursuit policy for guaranteed capture of intruder in minimum time. The major contributions of this paper are as follows:

(a) Guaranteed faster capture than previous results, due to additional information from the LFS.
(b) Expanded feasible capture region where guaranteed capture is possible because of LFS.
(c) Establishing the minimum number of columns of LFS to achieve (a) and (b). We establish the minimum number of LFS columns that is sufficient to catch the intruder when the pursuit starts with a finite initial delay.
The maximum initial delay with a capture guarantee can then be used as a specification for designing LFS structures in any practical scenario of guarding a border with the aid of UVs.
(d) Showing that additional UVs will not improve performance than that obtained by two UVs pursuing one intruder with any number of rows.

3. Modeling of Participating Elements

3.1. *Terrain model*

The long border is partitioned into a finite number of rows and infinite columns. For a partitioning of border into three rows and infinite columns, the rows are named as top (t), center (c) and bottom (b) and columns are numbered sequentially from 1 to n (refer Fig. 2).

Each space in the partitioned sector is named as a cell and it is identified as $C(r(\cdot), c(\cdot))$, where $r \in \{t, c, b\}$ and $c \in \{1, 2, \ldots, n\}$. Each of the cell is equipped with UGSs that can detect intruder movement. Some cells may have a LFSs and are placed along any or all sides of a cell that can detect intruder's direction of motion. Segmentation of number of rows and columns of a given terrain depends on the mission requirements, sensor characteristics (of UGS and LFS) and pursuer's behavior.

3.2. *Laser fence system*

A UGS positioned at the center of each cell can detect the intruder's movement at any point within the cell. The cellular grid structure additionally has laser fences along the columns, enabling additional information on intruder's direction of movement.

Let C_{sl} indicate the binary flag of a UGS with its adjacent LFS; $C_{sl} = 1$ indicates availability of information in UGS from LFS and $C_{sl} = 0$ otherwise. Triggering status of the laser fence is denoted by the binary variable L: $L = 1$ indicates that laser fence is triggered and $L = 0$ otherwise. If an intruder I enters the cell containing the ith UGS at the mth time instant, the corresponding LFS is triggered when the intruder crosses the laser fence at $(m+1)$th time instant. Upon triggering, the intruder information $\mathcal{I}nfo(I)$ from the laser fence becomes available to the immediately preceding ith UGS — namely, the time instant $m+1$ at which the laser fence is crossed by intruder I, and the ith cell from which the corresponding laser fence is crossed; this would provide directional information about the movement of the intruder. If $\delta(\cdot)$ indicates the discrete Dirac delta function, the following represents a functional model of LFS:

$$\mathcal{I}_l(m+1) = \mathcal{I}nfo(I)\delta(L-1)\delta(C_{sl}-1), \tag{1}$$

where $\mathcal{I}_l(m+1)$ is the information available in ith UGS due to LFS trigger and $\mathcal{I}nfo(I)$ is intruder information with time stamp.

3.3. *Unattended ground sensors*

An UGS considered in this work is basically a smart sensor having the following capabilities: (a) to detect any intruder moving within its sensing range, (b) to store the time at which the intruder is detected, (c) to establish contact with neighboring LFS, (d) to establish contact with UV and (e) to share with UV, the time lapsed since detection of intruder and intruder's direction of movement.

Let R_s be the sensing range of a UGS, R_{sf} be the communication range between a UGS and a LFS and R_{su} be the communication range between a UGS and a UV.

During the sensor placement, LFS is positioned such that its distance from the nearest UGS is within R_{sf} and hence C_{sl} with any UGS and its nearest LFS is always ON (1) unless there is any communication failure between them.

At each discrete step, the intruder I takes actions from a predefined action set and moves in discrete space; the position of the intruder is given by coordinates $C(r(.), c(.))$, where $r \in \{t, c, b\}$ and $c \in \{1, 2, \ldots, n\}$. UGS and LFS get triggered based on the intruder movement. The triggered UGS collects the information directly from its sensing system and from nearest triggered (i.e. $L = 1$) laser fencing system and stores these intruder information $\mathcal{I}nfo(I)$ with time stamp. The following equation represents functional model of ith UGS:

$$\mathcal{I}_{s_i}(m) = \mathcal{I}nfo(I), \quad \text{when} d(s_i, I) \leq R_s, \tag{2}$$

$$\mathcal{I}_{l_i}(m+1) = \mathcal{I}nfo(I)\delta(L-1)\delta(C_{sl}-1), \tag{3}$$

$$\mathcal{I}_{s_i}(m+1) = \{\mathcal{I}_{s_i}(m), \mathcal{I}_{l_i}(m+1)\}, \tag{4}$$

where $\mathcal{I}_{s_i}(m)$ is the information available at time instant m in ith UGS due to UGS trigger, $\mathcal{I}_{l_i}(m+1)$ is the information available at time instant $m+1$ in ith UGS due to corresponding LFS trigger and $\mathcal{I}_{s_i}(m+1)$ is the total information available at time instant $m+1$ in ith UGS. At kth time instant $(k \geq m)$, information sharing to the pursuer UV is based on the following model:

$$\mathcal{I}_u(k) = \{I_{s_i}(k), k-m\}, \quad \text{when } d(s_i, U) \leq R_{su}, \tag{5}$$

where $\mathcal{I}_u(k)$ is the information shared to the pursuer UV along with time lapse $(k-m)$, when UGS is interrogated.

4. Assumptions

The following are the standing assumptions made throughout the paper:

(a) The layout of the grid network, the placement of the UGS and LFS is known to pursuers, namely, the UVs.
(b) UGS detects when intruder passes by, stores the information along with time stamp, and when UVs comes in contact within UGS communication radius, it shares this information to UVs.
(c) LFS detects when intruder passes by, stores the information along with time stamp, shares with neighboring UGS, and when UVs comes in contact within communication radius of UGS, it shares this additional information to UVs.
(d) UVs travels from one cell to neighboring cell in one time step whereas intruder takes two time steps to travel between neighboring cells. The models we consider is applicable to ground robots or vehicles, that move between neighboring nodes.
(e) The intruder shall always be on the move and is constrained not to visit any cell more than once.

5. Pursuit-Evasion in a Cellular Structure

Consider a cellular structure consisting of an infinite number of columns and three rows, identified by the letter t for the top row, c for the center row and b for the bottom row. The columns are numbered from the left to the right as $0, 1, 2, \ldots$, etc. We denote the coordinates of a grid point by (r, i), where $r \in \{t, c, b\}$ indicates the row and $i = 0, 1, 2, \ldots$ denotes the column number. The grid points are the nodes of the network and the horizontal and vertical connecting roads are the edges. At time k, the allowed actions for the intruder at a cell are indicated by $w(k) \in \{N, E, S\}$, where N, E and S indicate going North, East and South, respectively, provided a path exists in that direction. Note that Assumption (e) precludes cycles in the graph. Unlike the intruder, the pursuer is able to wait at a cell. So, the allowed pursuer actions at time k are given by $u(k) \in \{N, E, S, L\}$, where L indicates loitering/waiting at the same node location until the next time step.

5.1. *Pursuer–intruder dynamics*

Let the pursuer's state, i.e. location on grid, at time k, be denoted by $p(k) = (r_p(k), i_p(k))$, follow the discrete-time dynamics:

$$p(k+1) = f_p(p(k), u(k)), \quad u(k) \in \mathcal{U}(r_p(k)), \tag{6}$$

where $\mathcal{U}(r_p(k))$ is the set of allowed actions from row $r_p(k)$. In particular,

$$\begin{aligned} &\mathcal{U}(b) = \{N, E, L\}, \quad \mathcal{U}(t) = \{S, E, L\} \quad \text{and} \\ &\mathcal{U}(c) = \{N, S, E, L\}. \end{aligned} \tag{7}$$

Let the intruder's state at time k be denoted by $e(k) = (p_e(k), o_e(k))$, where $p_e(k) = (r_e(k), i_e(k))$ is its position on the grid and $o_e(k) \in \{N, E, S\}$ is its current orientation/heading. Let the intruder's state follow the discrete-time dynamics:

$$e(k+2) = f_e(e(k), w(k)), \quad w(k) \in \mathcal{W}(p_e(k), o_e(k)), \tag{8}$$

where $\mathcal{W}(p_e(k), o_e(k))$ is the set of allowed intruder actions from the state $e(k)$. We retain the intruder's orientation, in addition to its location, so as to enforce additional motion constraints, such as preventing the intruder from making a U-turn, and so, we have

$$\begin{aligned} &\mathcal{W}(b, S) = \mathcal{W}(t, N) = \{E\}, \\ &\mathcal{W}(b, E) = \mathcal{W}(c, N) = \{N, E\}, \\ &\mathcal{W}(c, S) = \mathcal{W}(t, E) = \{S, E\} \quad \text{and} \\ &\mathcal{W}(c, E) = \{N, S, E\}. \end{aligned} \tag{9}$$

Also, we increment time by 2 in (8), so as to indirectly impose the $2\times$ speed advantage of the pursuer.

Recall that the pursuer, upon arriving at a grid point, interrogates the UGS at that location and makes one of two observations: status "red" with delay $D \geq 0$ indicating that the intruder was at that location D time steps ago or status "green" indicating that the location has not been visited by the intruder. So, we denote the observation made by the pursuer at time k by

$$z(k) = \begin{cases} D & \text{if } p_e(k-D) = p(k), \text{for some } D \in [0,k], \\ G & \text{otherwise.} \end{cases} \tag{10}$$

Here, G indicates "green" status of the UGS at $p(k)$. Note that $z(k)$ is an *implicit* function of k as it is a function of the current location of the pursuer $p(k)$, and the trajectory of the intruder until time k, i.e. $\{p_e(k-j), j \geq 0\}$. Although the intruder's trajectory is unknown, the pursuer can infer the possible locations of the intruder through the observations it made: $z(0), \ldots, z(k)$. For convenience, we shall denote the position of the pursuer and the observation made at time k together by the augmented state, $x_p(k) = (p(k), z(k)) = (r(k), i(k), z(k))$, to indicate that the pursuer is at row $r(k)$, column $i(k)$ and has made the observation $z(k)$ at time k.

6. Optimization Problem

Suppose the intruder is at the location (r, i_0) at time 0. After some delay $D > 0$, the pursuer arrives (for the first time) at the same location (r, i_0), knowing that the intruder entered (r, i_0) from outside the grid, see Fig. 3, and is tasked with capturing the intruder. We are interested in a pursuit policy that will lead to capture at the earliest, for the worst possible intruder trajectory. Since the pursuer has no direct knowledge of the intruder's position, except the information it gathered from the UGSs, we define the information state of the pursuer at time $k \geq D$ by: $\mathcal{I}(k) = (x_p(D), \ldots, x_p(k))$, i.e. the locations it has visited thus far, and the observations made there. Let $\mathcal{A}$ denote the set of all admissible control polices, where an admissible control policy $A \in \mathcal{A}$ is a sequence of maps from the information state $\mathcal{I}(k)$ to the set of control actions available at the current pursuer location, $\mathcal{U}(r_p(k))$.

Let $J(r, D, A, w(2k); k \geq 0)$ be the number of steps to capture, when the pursuer starts from the augmented state, $x_p(D) = (r, i_0, D)$ and executes the control policy, $A : u(k) = A(\mathcal{I}(k))$; $k \geq D$, thereafter, while the intruder implements the actions, $w(2k)$; $k \geq 0$. If capture never occurs, we set J to ∞.

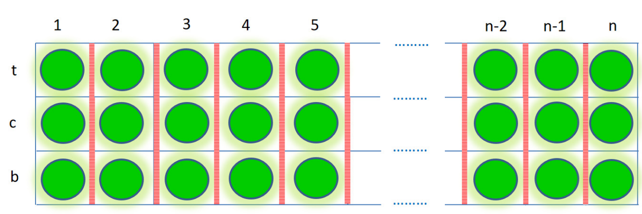

Fig. 3. Cellular network with LFS.

Definition 6.1. For any $A \in \mathcal{A}$, define

$$T_A(r, D) = \sup_{\substack{w(2k) \in \mathcal{W}(e(2k)) \\ k = 0,1,\ldots}} J(r, D, A, w(2k); k \geq 0). \tag{11}$$

Definition 6.2. The worst-case minimum time to capture is then given by

$$\begin{aligned} T(r, D) &= \min_{A \in \mathcal{A}} \sup_{\substack{w(2k) \in \mathcal{W}(e(2k)) \\ k = 0,1,\ldots}} J(r, D, A, w(2k); k \geq 0) \\ &= \min_{A \in \mathcal{A}} T_A(r, D). \end{aligned} \tag{12}$$

For any policy $A \in \mathcal{A}$, we also define $A_{r,D}$ to be its restriction to the initial augmented state: $x_p(D) = (r, i_0, D)$. To be clear, the restriction $A_{r,D}$ only specifies (completely) what the pursuer should do starting from the augmented state, $x_p(D)$ and thereafter, for all possible future augmented states, until the intruder is captured.

6.1. *Dynamic programming solution*

Suppose at time $k > D$, the intruder is yet to be captured and we are interested in obtaining the min–max steps to capture thereafter. Let $V^*(\mathcal{I})$ denote the minimum time (or number of pursuer's steps) for guaranteed interception of the intruder with the information state $\mathcal{I}$. We note that the information state evolves according to

$$\mathcal{I}(k+1) = (\mathcal{I}(k), f_p(p(k), u(k)), z(k+1)), \tag{13}$$

which shows the explicit dependence on the future course of action of, and the likely observations made, by the pursuer. Then, one can write the following Dynamic Programming (DP) recursion to obtain $V^*(\mathcal{I}(k))$:

$$V^*(\mathcal{I}(k)) = 1 + \min_{u(k)} \max_{\mathcal{I}(k+1) \in \mathbf{I}(\mathcal{I}(k), u(k))} V^*(\mathcal{I}(k+1)), \tag{14}$$

where $\mathbf{I}(\mathcal{I}(k), u(k))$ denotes the set of all possible information states at $k+1$ that satisfy (13) for a given $\mathcal{I}(k)$ and $u(k)$.

By definition, we have $T(r, D) = V^*(\mathcal{I}(D))$ and so, one can obtain $T(r, D)$ and the corresponding optimal pursuit policy $A^* \in \mathcal{A}$ by solving the recursion (14). It becomes readily apparent that the DP method quickly becomes intractable for large delays D, unless some structure in the problem is exploited. This is primarily due to the explosion in the number of pursuer and intruder paths that one has to consider and the partial and delayed information structure, i.e. the information state grows unbounded with time. Luckily, the problem exhibits structure characterized by the translational and reflection symmetry in the Manhattan grid and motion constraints imposed on the pursuer and intruder. These enable us to *indirectly* solve the DP recursion in an efficient manner. Indeed, we arrive at a induction-based solution method that works for any delay, $D \geq 3$. For smaller delays $D < 3$, we deduce the optimal strategy and the corresponding time to capture, by explicit enumeration.

7. Optimal Solution to Minimum Time Capture Problem

In this section, we shall first show that on the grid depicted in Fig. 3, the minimum time to capture under worst-case intruder action, is bounded.

We shall do so by demonstrating that there exists a policy $\mu \in \mathcal{A}$ such that

$$T_1^b(\mu) = 1, \quad T_2^b(\mu) = 2, \tag{15}$$

$$T_D^b(\mu) = D + 4, \quad \forall\, D \geq 3 \quad \text{and} \tag{16}$$

$$T_D^c(\mu) = D + 4, \quad \forall\, D > 0. \tag{17}$$

Since the optimal policy can do no worse than the policy μ, we have $T_D^r \leq T_D^r(\mu)$, $r \in \{b, c\}$. Note that, due to the symmetry of the graph (see Fig. 3) and in the allowed set of actions for the pursuer and intruder, $T_D^t = T_D^b$, and so, there is no need to consider the top row cases separately. The restriction of the policy μ to all the cases, referred to as $\mu_{r,D}$, is specified as follows until the intruder is captured:

- Pursuer follows intruder path from red UGS, whenever direction of intruder's move is known.
- Otherwise, pursuer goes "north" from red UGS, without loss of generality. However, it can be easily shown that a random policy (by tossing a coin to go N or S) will result in the same performance.
- From green UGS, at the top row at the first column, pursuer goes "east".
- From green UGS, at the top row at the second column, pursuer goes "south".
- From green UGS, at the central row at the second and subsequent columns, pursuer goes "south" if only delay D becomes 1 or 2 there; or "east".
- At bottom row whenever delay D becomes 2, pursuer follows intruder.

Lemma 7.1. *There exists a pursuit policy* μ, *such that* $T_1^b(\mu) = 1$.

Proof. This is the scenario where the pursuer arrives at a red UGS with delay $D = 1$ in the bottom row, i.e. $x_p(1) = (b, 1, 1)$ — see column 1 of Fig. 4. For the policy μ, as defined so far, Table 1 lists the different times at which capture will occur, the augmented pursuer state at that time and the corresponding steps to capture, for all possible intruder strategies.

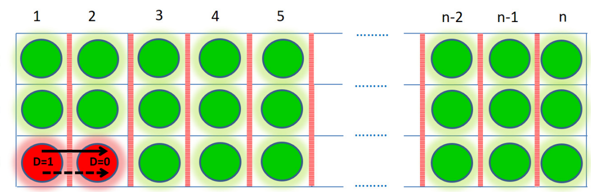

Fig. 4. Bottom row, initial delay $D = 1$.

Table 1. $T_1^b(\mu)$: Steps to capture for different intruder strategies.

Intruder strategy	Time (k)	$x_p(k)$	Steps
E	2	$(b, 2, 0)$	1
N	2	$(c, 1, 0)$	1

The worst-case sequence of intruder moves, $W_{b,1} = E$ or N leads to capture in 1 step, under pursuit policy μ, and so, $T_1^b(\mu) = 1$. The corresponding trajectory for both parties along with the UGS statuses (green or red with delay) encountered by the pursuer are shown in Fig. 4 — columns numbered 1 and 2, where dotted arrows indicate the pursuer path, and solid arrows indicate the intruder path. □

Lemma 7.2. *There exists a pursuit policy* μ, *such that* $T_2^b(\mu) = 2$.

Proof. This is the scenario where the pursuer arrives at a red UGS with delay $D = 2$ in the bottom row, i.e. $x_p(2) = (b, 1, 2)$ — see column 1 of Fig. 5.

For the policy μ, as defined so far, Table 2 lists the different times at which capture will occur, the augmented pursuer state at that time and the corresponding steps to capture, for all possible intruder strategies.

The worst-case sequence of intruder moves, $W_{b,2} = E$, then follow $W_{b,1}$ or NE or N^2 leads to capture in two steps,

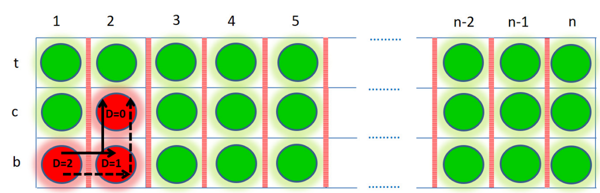

Fig. 5. Bottom row, initial delay $D = 2$.

Table 2. $T_2^b(\mu)$: Steps to capture for different intruder strategies.

Intruder strategy	Time (k)	$x_p(k)$	Steps
$E * W_{b,1}$	3	$(b, 2, 1)$	2
NE	4	$(c, 2, 0)$	2
N^2	4	$(t, 1, 0)$	2

January 5, 2022 1:47:43pm WSPC/284-US 2250005 ISSN: 2301-3850 2nd Reading

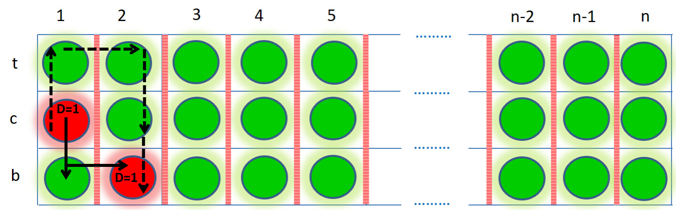

Fig. 6. Central row, initial delay $D = 1$.

Table 3. $T_1^c(\mu)$: Steps to capture for different intruder strategies.

Intruder strategy	Time (k)	$x_p(k)$	Steps
E	2	$(c, 2, 0)$	1
N	2	$(t, 1, 0)$	1
$SE * W_{b,1}$	5	$(b, 2, 1)$	5

under pursuit policy μ, and so, $T_2^b(\mu) = 2$. The corresponding trajectory for both parties along with the UGS statuses (green or red with delay) encountered by the pursuer are shown in Fig. 5 — columns numbered 1 and 2, where dotted arrows indicate the pursuer path, and solid arrows indicate the intruder path. □

Lemma 7.3. *There exists a pursuit policy μ, such that $T_1^c(\mu) = 5$.*

Proof. This is the scenario where the pursuer arrives at a red UGS with delay $D = 1$ in the central row, i.e. $x_p(2) = (c, 1, 1)$ — see column 1 of Fig. 6.

For the policy μ, as defined so far, Table 3 lists the different times at which capture will occur, the augmented pursuer state at that time and the corresponding steps to capture, for all possible intruder strategies.

The worst-case sequence of intruder moves, $W_{c,1} = SE$, then follow $W_{b,1}$ leads to capture in five steps, under pursuit policy μ, and so, $T_1^c(\mu) = 5$.

The corresponding trajectory for both parties along with the UGS statuses (green or red with delay) encountered by the pursuer are shown in Fig. 6 — columns numbered 1 and 2, where dotted arrows indicate the pursuer path, and solid arrows indicate the intruder path. □

Lemma 7.4. *There exists a pursuit policy μ, such that $T_2^c(\mu) = 6$.*

Proof. This is the scenario where the pursuer arrives at a red UGS with delay $D = 2$ in the central row, i.e. $x_p(2) = (c, 1, 2)$ — see column 1 of Fig. 7.

For the policy μ, as defined so far, Table 4 lists the different times at which capture will occur, the augmented pursuer state at that time and the corresponding steps to capture, for all possible intruder strategies.

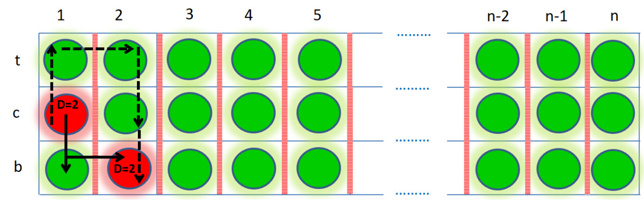

Fig. 7. Central row, initial delay $D = 2$.

Table 4. $T_2^c(\mu)$: Steps to capture for different intruder strategies.

Intruder strategy	Time (k)	$x_p(k)$	Steps
$E * W_{c,1}$	3	$(c, 2, 1)$	6
NE	4	$(t, 2, 0)$	2
$SE * W_{b,2}$	6	$(b, 2, 2)$	6

The worst-case sequence of intruder moves, $W_{c,2} = E$, then follow $W_{c,1}$ or SE, then follow $W_{b,2}$ leads to capture in six steps, under pursuit policy μ, and so, $T_2^c(\mu) = 6$. The corresponding trajectory for both parties along with the UGS statuses (green or red with delay) encountered by the pursuer are shown in Fig. 7 — columns numbered 1 and 2, where dotted arrows indicate the pursuer path, and solid arrows indicate the intruder path. □

From the pursuit strategies that arose in the cases considered thus far, an inductive argument appears to emerge for bigger delays. Indeed, we shall specify the remainder of the policy μ for delays $D \geq 3$ and demonstrate the following general result.

Theorem 7.5. *Suppose $D \geq 3$. Then,*

$$T_D^r(\mu) = D + 4, \quad r \in \{b, c\}. \tag{18}$$

Proof. We shall prove the result via mathematical induction.

Basic step. We will show that the result holds for $D = 3$.

Case (a). First, we show that $T_3^b(\mu) = 7$.

In this scenario (see Fig. 8), the pursuer arrives at a red UGS with delay 3 in the bottom row, i.e. $x_p(3) = (b, 1, 3)$ — see column 1 of Fig. 8.

For the policy μ, as defined so far, Table 5 lists the different times at which capture will occur, the augmented

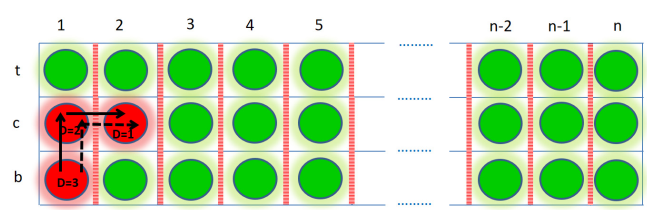

Fig. 8. Bottom row, initial delay $D = 3$.

January 5, 2022 1:47:52pm WSPC/284-US 2250005 ISSN: 2301-3850 2nd Reading

Table 5. $T_3^b(\mu)$: Steps to capture for different intruder strategies.

Intruder strategy	Time (k)	$x_p(k)$	Steps
$E * W_{b,2}$	4	$(b, 2, 2)$	3
$NE * W_{c,1}$	5	$(c, 2, 1)$	7
N^2E	6	$(t, 2, 0)$	3

pursuer state at that time and the corresponding steps to capture, for all possible intruder strategies.

The worst-case sequence of intruder moves, $W_{b,3} = NE$, then follow $W_{c,1}$ leads to capture in seven steps, under pursuit policy μ, and so, $T_3^b(\mu) = 7$.

The corresponding trajectory for both parties along with the UGS statuses (green or red with delay) encountered by the pursuer are shown in Fig. 8 — columns numbered 1 and 2, where dotted arrows indicate the pursuer path, and solid arrows indicate the intruder path.

Case (b). We now proceed to show that $T_3^c(\mu) = 7$. In this scenario (see Fig. 9), the pursuer arrives at a red UGS with delay 3 in the center row, i.e. $x_p(3) = (c, 1, 3)$ — see column 1 of Fig. 9.

For the policy μ, as defined so far, Table 6 lists the different times at which capture will occur, the augmented pursuer state at that time and the corresponding steps to capture, for all possible intruder strategies.

The worst-case sequence of intruder moves, $W_{c,3} = E$, then follow $W_{c,2}$ or SE^2, then follow $W_{b,2}$ leads to capture in seven steps, under pursuit policy μ, and so, $T_3^c(\mu) = 7$.

The corresponding trajectory for both parties along with the UGS statuses (green or red with delay) encountered by the pursuer are shown in Fig. 9 — columns numbered 1, 2 and 3, where dotted arrows indicate the pursuer path, and solid arrows indicate the intruder path.

Induction step. For $r \in \{b, c\}$, we recursively define the restrictions, $\mu_{r,D}$, $D \geq 4$, to the policy, μ, as follows: for the

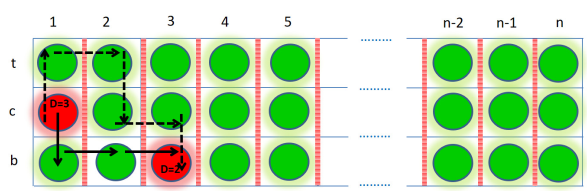

Fig. 9. Central row, initial delay $D = 3$.

Table 6. $T_3^c(\mu)$: Steps to capture for different intruder strategies.

Intruder strategy	Time (k)	$x_p(k)$	Steps
$E * W_{c,2}$	4	$(c, 2, 2)$	7
$NE * W_{t,1}$	5	$(t, 2, 1)$	3
SEN	6	$(b, 2, 0)$	3
$SE^2 * W_{b,2}$	8	$(b, 3, 2)$	7

case $r = b$, the pursuer follows intruder's move as direction of intruder's move is known until either the intruder is captured or a red UGS is encountered with a lower delay, whichever occurs first, and for the case $r = c$, the pursuer executes either the sequence of actions $NESE^{D-2}S * U_{b,2}$ until the intruder is captured, if intruder's first move is not E, or $E * U_{c,D-1}$ otherwise. If a red observation is encountered at row $\bar{r}$ with delay $\bar{D}$, the pursuer will switch to the policy specified by $\mu_{\bar{r},\bar{D}}$. Note that the policy corresponding to $\bar{r} = t$ is a mirror image of the policy obtained for $\bar{r} = b$ and can be obtained by swapping N for S and vice-versa in $\mu_{b,\bar{D}}$.

This completes the specification of the policy μ.

Assume that for some $D \geq 4$,

$$T_M^r(\mu) = M + 4, \quad M = 3, \ldots, (D-1), \quad r \in \{b, c\}. \quad (19)$$

We proceed to show that $T_D^r(\mu) = D + 4$.

Case (a). First, we show that $T_D^c(\mu) = D + 4 \; \forall \; D \geq 4$.

For the policy μ, as defined so far, Table 7 lists the different times at which capture will occur, the augmented pursuer state at that time and the corresponding steps to capture, for all possible intruder strategies.

The worst-case sequence of intruder moves, $W_{c,D:D\geq 4} = E$, then follow $W_{c,D-1}$ or NE, then follow $W_{t,D-2}$ or SE^{D-1}, then follow $W_{b,2}$ leads to capture in $D + 4$ steps, under pursuit policy μ, and so, $T_D^c(\mu) = D + 4$.

The corresponding trajectory for both parties along with the UGS statuses (green or red with delay) encountered by the pursuer for intruder strategy $SE^{D-1} * W_{b,2}$ are shown in Fig. 10 — columns numbered 1 to D, where dotted arrows

Table 7. $T_D^c(\mu) \; \forall \; D \geq 4$: Steps to capture for different intruder strategies.

Intruder strategy	Time (k)	$x_p(k)$	Steps
$E * W_{c,D-1}$	$D + 1$	$(c, 2, D-1)$	$D + 4$
$NE * W_{t,D-2}$	$D + 2$	$(t, 2, D-2)$	$D + 4$
$SENE * W_{c,D-4}$	$D + 4$	$(c, 3, D-4)$	$D + 4$
$SEN^2E * W_{t,D-7}$	$D + 3$	$(t, 3, D-7)$	D
$SE^2NE * W_{c,D-5}$	$D + 5$	$(c, 4, D-5)$	$D + 4$
$SE^2N^2E * W_{t,D-6}$	$D + 6$	$(t, 4, D-6)$	$D + 4$
$\vdots$	$\vdots$	$\vdots$	$\vdots$
$SE^{D-1} * W_{b,2}$	$2D + 2$	$(b, D, 2)$	$D + 4$

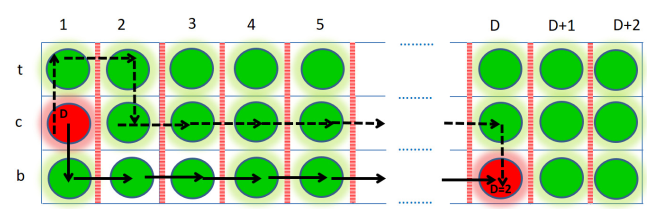

Fig. 10. Central row, initial delay $D \geq 4$.

Table 8. $T_D^b(\mu)\ \forall\ D \geq 4$: Steps to capture for different intruder strategies.

Intruder strategy	Time (k)	$x_p(k)$	Steps
$E * W_{b,D-1}$	$D+1$	$(b, 2, D-1)$	$D+4$
$NE * W_{c,D-2}$	$D+2$	$(c, 2, D-2)$	$D+4$
$N^2E * W_{t,D-3}$	$D+3$	$(t, 2, D-3)$	$D+4$

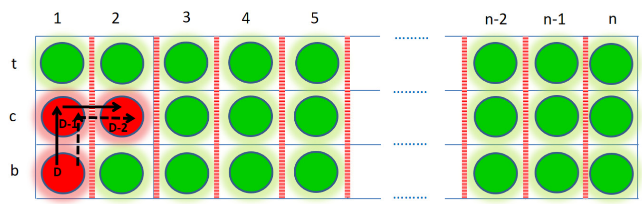

Fig. 11. Bottom row, initial delay $D \geq 4$.

indicate the pursuer path, and solid arrows indicate the intruder path.

Case (b). We now proceed to show that $T_D^b(\mu) = D + 4\,\forall\, D \geq 4$.

For the policy μ, as defined so far, Table 8 lists the different times at which capture will occur, the augmented pursuer state at that time and the corresponding steps to capture, for all possible intruder strategies.

The worst-case sequence of intruder moves, $W_{b,D:D\geq 4} = E$, then follow $W_{b,D-1}$ or NE, then follow $W_{c,D-2}$ or N^2E, then follow $W_{t,D-3}$ leads to capture in $D+4$ steps, under pursuit policy μ, and so, $T_D^b(\mu) = D+4$.

The corresponding trajectory for both parties along with the UGS statuses (green or red with delay) encountered by the pursuer for intruder strategy $NE * W_{c,D-2}$ are shown in Fig. 11, where dotted arrows indicate the pursuer path, and solid arrows indicate the intruder path. □

Since the optimal policy can do no worse than the policy μ, we have from Lemmas 7.1–7.4 and Theorem 7.5:

$$T_1^b \leq 1, \quad T_2^b \leq 2, \tag{20}$$

$$T_D^b \leq D+4, \quad \forall D \geq 3 \quad \text{and} \tag{21}$$

$$T_D^c \leq D+4, \quad \forall D > 0. \tag{22}$$

We shall now proceed to show that μ is an optimal pursuit policy.

In order to prove the optimality of μ, it suffices to show that $T_1^b \geq 1, T_2^b \geq 2$, $T_D^b \geq D+4, \forall\ D \geq 3$ and $T_D^c \geq D+4$, $\forall\ D \geq 1$. The basic idea behind the construction of the lower bound is the following:

- If one were to restrict the set of trajectories of the intruder in (12) by requiring $w(2k) \in \hat{\mathcal{W}}(e(2k)) \subset \mathcal{W}(e(2k))$, one gets a lower bound for T_D^r. Essentially, this is tantamount to optimizing the pursuer's policy over a restricted set of intruder trajectories.

In order to facilitate the optimization over pursuer policies, we provide Lemmas 7.6 and 7.7.

Lemma 7.6. *If pursuer is at (r_i, c_i) and it knows that intruder is at (r_j, c_j), where $c_j \geq c_i$; then the time to capture intruder from that condition,* $T \geq 2(|r_i - r_j| + c_j - c_i)$.

Proof. In this scenario, intruder has always free passage to go away from pursuer, i.e. pursuer cannot confine intruder in a corner. There will be many uncertainties, if pursuer takes any step except coming to intruder's known position and follow it. The case is exactly same as chasing intruder in a one row infinite column cells from behind. $|r_i - r_j| + c_j - c_i$ time is taken to come to known position of intruder. By that time intruder will move further, and it will take another $|r_i - r_j| + c_j - c_i$ time to capture under full information. Therefore, time to capture intruder from initial condition under this policy is $2(|r_i - r_j| + c_j - c_i)$ and so $T \geq 2$ $(|r_i - r_j| + c_j - c_i)$. □

Lemma 7.7. *It is optimal for pursuer to follow intruder from a red UGS location, whenever direction of intruder's move is known to be east.*

Proof. Suppose the intruder enters a location (r, i_0) at some time and let $\mathcal{I}_0$ be the information available to a pursuer occupying the same location $D \geq 1$ time units later. Because of speed advantage, in one move pursuer at best can only reduce the delay by 1. Therefore, it is always optimal to follow intruder when direction of move is known to be east as it reduces the delay by 1. □

Lemma 7.8. *Suppose the pursuer's initial augmented state is $x_p(D) = (r, i_0, D)$. Then, we have*

$$T_D^r \geq D - 3 + T_3^r, \quad \forall D \geq 4.$$

Proof. Suppose we restrict the set of intruder's trajectories to contain the segment E^{D-3} starting at the red UGS location at (r, i_0), i.e. $w(2k) = E$, $k = 1, 2, \ldots, D-3$. Let $\hat{T}_D^r$ denote the worst-case, minimum time to capture, when the intruder's trajectories are restricted in the manner specified. By definition (12), the worst-case minimum time to capture, $T_D^r \geq \hat{T}_D^r$. From Lemma 7.7, there exists an optimal pursuit policy, B, such that $B(\mathcal{I}(D)) = E$. By following the policy B, under the restriction, the pursuer will encounter another red UGS with delay $D-1$ at time $D+1$. So, by repeated application of Lemma 7.7, the optimal action for the pursuer is to go east at every one of the subsequent $D-3$ red UGS locations; until at time $2D-3$, it encounters a red UGS with delay 3. Hence, $\hat{T}_D^r = D - 3 + T_3^r$. Since $T_D^r \geq \hat{T}_D^r$, the result follows. □

Lemma 7.9. *The worst-case minimum number of steps to capture, for delays* $D <= 3$ *are given by*

$$T_1^b = 1, \quad T_2^b = 2, \quad T_3^b = 7 \quad \text{and} \\ T_D^c = D + 4, \quad D = 1, 2, 3. \tag{23}$$

Proof. $T_1^b \geq 1$ and $T_2^b \geq 2$, as 1 and 2 are the lower bound for T_1^b and T_2^b. This is because of the fact that D is the lowest possible capture time with D delay because of the speed advantage of pursuer, in one move pursuer at best can only reduce the delay by 1. From Lemma 12, we have $T_1^b \leq 1$ and $T_2^b \leq 2$, it follows that $T_1^b = 1$ and $T_2^b = 2$.

Let us see the case of T_D^c for $D = 1, 2, 3$. From the Figures 6, 7, 9, it is seen that after D steps, the Manhattan distance between pursuer and intruder becomes 2, so from Lemma 7.7, $T_D^c \geq D + 4$. From Lemma 12, we have $T_D^c \leq D + 4$, it follows that $T_D^c = D + 4 \ \forall \ D = 1, 2, 3$.

For case of T_3^b, after two steps, it becomes T_1^c case. So, $T_3^b \geq 2 + T_1^c = 7$. From Lemma 12, we have $T_3^b \leq 7$, it follows that $T_3^b = 7$. □

Theorem 7.10. *The worst-case minimum number of steps to capture, starting from any row* r *with delay* $D \geq 3$,

$$T_D^r = D + 4, \quad \forall \ r \in \{t, c, b\},$$

and μ *is an optimal policy.*

Proof. By combining Lemmas 7.8 and 7.9, we readily obtain,

$$T_D^r \geq D - 3 + T_3^r = D + 4, \quad D \geq 4.$$

From Theorem 7.5, we have $T_D^r \leq D + 4, \forall \ D \geq 3$. So, From Lemmas 7.8, 7.9 and Theorem 7.5, $T_D^r = D + 4, \forall \ D \geq 3$. It follows that the policy μ, specified earlier, is optimal. □

8. Optimal Solution to Minimum Time Capture Problem with Four Rows

It is not possible to capture intruder for all possible and admissible moves of intruder by any particular pursuit policy in four-row case with UGS only. But with additional information due to laser fencing, capture becomes possible. The restriction of the policy μ to all the cases, referred to as $\mu_{r,D}$, is specified in similar way as follows: the pursuer either follows intruder whenever direction of intruder's move is known, or goes "North (N)", until the intruder is captured for bottom two rows. For convenience, the bottom two rows will be referred as "b" and "c". As will be seeing, the four row capture case is possible because the extra information from the LFS allows the UV to cordon off the intruder into three rows, making the four-row case degenerates into a three-row problem. The pursuit policy is exactly the same as that of three-row case.

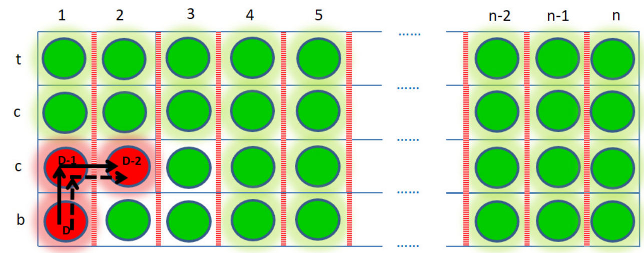

Fig. 12. Bottom row, initial delay $D \geq 3$.

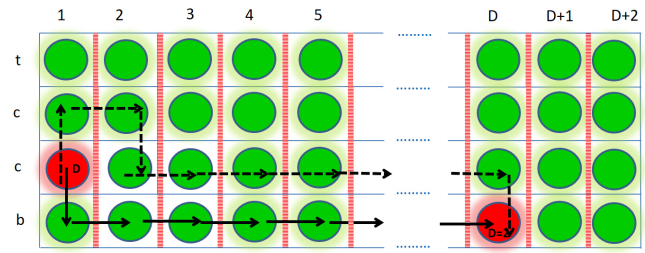

Fig. 13. Central row, initial delay $D \geq 3$.

It can be shown that on the Manhattan grid depicted in Figs. 12 and 13, the minimum time to capture under worst-case intruder action, is as follows:

$$T_1^b(\mu) = 1, \quad T_2^b(\mu) = 2, \tag{24}$$

$$T_D^b(\mu) = D + 4, \quad \forall \ D \geq 3 \quad \text{and} \tag{25}$$

$$T_D^c(\mu) = D + 4, \quad \forall \ D > 0. \tag{26}$$

Since the optimal policy can do no worse than the policy μ, we have $T_D^r \leq T_D^r(\mu), r \in \{b, c\}$. As the capture time under policy μ for four-row case is same as that for three-row case, the policy μ is the optimal policy. Note that, due to the symmetry of the graph (see Figs. 12 and 13) and in the allowed set of actions for the pursuer and intruder, $T_D^t = T_D^b$, and so, there is no need to consider the top two-row cases separately. The LFS allows capture by one UV in the four-row case, previously unattainable with UGS alone, because of the extra information. This however is not possible with five rows, because when the intruder enters into the centre row, a pursuit policy does not exist that can reduce the delay after finite moves. Essentially, the uncertainty in the intruder's path cannot be reduced with the given information.

9. Optimal Solution to Minimum Time Capture Problem with Any Number of Rows and Two Pursuers

Consider a cellular network (see Fig. 14) consisting of an infinite number of rows and columns. The rows/columns are indexed by the set of nonnegative integers, $\mathcal{Z} = \{0, 1, 2, \ldots\}$.

January 5, 2022 1:48:07pm WSPC/284-US 2250005 ISSN: 2301-3850 2nd Reading

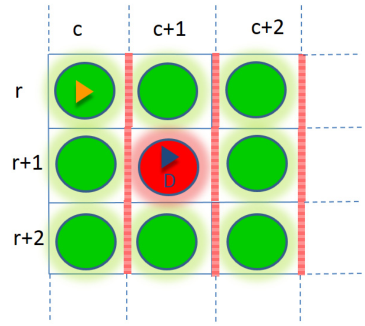

Fig. 14. Cellular network with two pursuers, and initial condition.

We denote the coordinates of a cell by (i,j), where i indicates the row and j denotes the column index. We assume that a pursuer travels from one cell to a neighboring cell in exactly one time step whereas the slower moving intruder takes two time steps to travel between neighboring cells.

At time k, the allowed actions for the intruder at a cell are indicated by $w(k) \in \{N, E, S\}$, where N, E and S indicate going North, East and South, respectively, provided a path exists in that direction. The intruder is constrained to be always on the move and also prohibited from visiting any given cell, more than once. This assumption precludes cycles in the graph and the ensuing intractability in solving the search problem. The pursuer, in addition to being able to move North (N), East (E) and South (S), can also wait at a node location. So, the allowed pursuer actions at time k are given by $u(k) \in \{N, E, S, L\}$, where L indicates loitering/waiting at the same node location until the next time step. Note that neither the pursuers nor the intruder can move west.

9.1. *Pursuer–intruder dynamics*

Let the mth pursuer's state, i.e. location on grid, at time k, denoted by $p_m(k) = (i_m(k), j_m(k))$, follow the discrete-time dynamics:

$$\begin{aligned} p_m(k+1) &= f_p(p_m(k), u_m(k)), \quad u_m(k) \in \mathcal{U}, \\ m &= 1, 2, \end{aligned} \tag{27}$$

where the allowed set of pursuer actions, $\mathcal{U} = \{N, S, E, L\}$. Let the intruder's state at time k be denoted by $e(k) = (p_e(k), o_e(k))$, where $p_e(k) = (i_e(k), j_e(k))$ is its position on the grid and $o_e(k) \in \{N, E, S\}$ is its current orientation/heading. Let the intruder's state follow the discrete-time dynamics:

$$e(k+2) = f_e(e(k), w(k)), \quad w(k) \in \mathcal{W}(o_e(k)), \tag{28}$$

where $\mathcal{W}(o_e(k))$ is the set of allowed intruder actions from the state $e(k)$. We retain the intruder's orientation, in addition to its location, so as to enforce additional motion constraints, such as preventing the intruder from making a U-turn, and so, we have

$$\mathcal{W}(N) = \{N, E\}, \quad \mathcal{W}(S) = \{S, E\} \quad \text{and}$$

$$\mathcal{W}(E) = \{N, S, E\}.$$

Also, we increment time by 2 in Eq. (28), so as to indirectly impose the $2\times$ speed advantage of the pursuer.

Recall that the pursuer, upon arriving at a grid point, interrogates the UGS at that location and makes one of two observations: status "red" with delay $D \geq 0$ indicating that the intruder was at that location D time steps ago or status "green" indicating that the location has not been visited by the intruder. So, we denote the observation made by the mth pursuer at time k by

$$z_m(k) = \begin{cases} \ell & \text{if } p_e(k-\ell) = p_m(k), \text{for some } \ell \in [0, k], \\ G & \text{otherwise}. \end{cases} \tag{29}$$

Here, G indicates "green" status of the UGS at $p_m(k)$.

9.2. *Optimization problem statement*

Suppose the intruder is at the location $(r+1, c+1)$ at time 0. After some delay $D > 0$, the first pursuer (colored dark blue) arrives (for the first time) at the same location $(r+1, c+1)$, knowing that the intruder entered $(r+1, c+1)$ from outside the grid — see Fig. 14. Further suppose that the second pursuer (colored orange) is at location (r, c), and the two are tasked with cooperatively capturing the intruder. We shall use $\mathcal{C}_D$ to denote this initial condition. There is no loss of generality here, since the pursuer who discovers the intruder for the first time (say pursuer 1) can always wait at the same location, until the other pursuer (say pursuer 2) arrives at the location immediately above and to the left of pursuer 1. Since the pursuers have no direct knowledge of the intruder's position, except the information they gathered from the UGSs, we define the information state at time $k \geq D$ by: $\mathcal{I}(k) = (x_p(D), \ldots, x_p(k))$, where $x_p(k) = (p_1(k), z_1(k), p_2(k), z_2(k))$, i.e. the locations visited thus far, and the observations made therein. Let $\mathcal{A}$ denote the set of all admissible control polices, where any $A \in \mathcal{A}$ is a (vector) sequence of maps from the information state $\mathcal{I}(k)$ to the available control actions, $\mathcal{U} \times \mathcal{U}$. Let $J(D, A, w(2k); k \geq 0)$ be the number of steps to capture, when the initial configuration is $\mathcal{C}_D$ and the pursuers' execute the control policy, $A : [u_1(k), u_2(k)] = A(\mathcal{I}(k))$; $k \geq D$, thereafter, while the intruder implements the actions, $w(2k); k \geq 0$. If capture never occurs, we set J to ∞.

Definition 9.1. For any $A \in \mathcal{A}$,

$$T_A(D) = \sup_{\substack{w(2k) \in \mathcal{W}(o_e(2k)) \\ k = 0, 1, \ldots}} J(D, A, w(2k); k \geq 0).$$

Definition 9.2. The worst-case minimum time to capture is then given by

$$T(D) = \min_{A \in \mathcal{A}} \sup_{\substack{w(2k) \in \mathcal{W}(o_e(2k)) \\ k=0,1,\ldots}} J(D, A, w(2k); k \geq 0)$$
$$= \min_{A \in \mathcal{A}} T_A(D).$$

For any policy $A \in \mathcal{A}$, we also define A_D to be its restriction to the initial delay: D. To be clear, the restriction A_D specifies (completely) what the pursuers should do starting from the configuration $\mathcal{C}_D$ and thereafter.

9.3. *Optimal solution*

In this section, we shall first show that on the cellular structure depicted in Fig. 14, the minimum time to capture under worst-case intruder action, is bounded. We shall do so by demonstrating that there exists a policy $\mu \in \mathcal{A}$ such that

$$T_D(\mu) = D, \quad \forall\, D \geq 1. \tag{30}$$

One of the two pursuers capture the intruder in D steps, in comparison to $D+4$ steps when there is no laser fencing. Henceforth, we shall distinguish the two (identical) pursuers as $P1$ and $P2$ to illustrate the collaborative pursuit policy. The cooperative policy μ is as follows:

- First move of $P2$ is always E. First move of $P1$ is either E, if laser is triggered along that direction or S otherwise.
- Second move of $P2$ is E, if laser is triggered along that direction or first move of $P1$ was E. Else, second move of $P2$ will be S or N depending on the fact that whether or not $P1$ encountered red UGS on its first move of S. Second move of $P1$ will be N in case $P2$ moves N.
- The above move logic will be recursively used till they either capture the intruder or reach a revised initial condition with a delay $D' < D$.

Since the optimal policy can do no worse than the policy μ, we have $T(D) \leq T_D(\mu), D > 0$.

Lemma 9.3. *There exists a pursuit policy μ, such that $T_1(\mu) = 1$.*

Proof. This is the scenario $\mathcal{C}_1$, where the first pursuer arrives at a red UGS at location $(r+1, c+1)$ with delay $D = 1$ (and second pursuer is at location (r, c)). The restriction of the policy μ to this case, referred to as μ_1, is specified as follows: First move of $P2$ is always E. First move of $P1$ is either E, if laser is triggered along that direction or S otherwise. Table 9 lists the time to capture, the capture location (and by whom), for all possible intruder strategies, when μ_1 is executed.

A worst-case sequence of intruder moves is given by $W_1 = \{N, E, S\}$ and the corresponding steps to capture as

Table 9. $\mathcal{C}_1$: Steps to capture for different intruder strategies.

Intruder strategy	Steps to capture	$p_e(k)$	Pursuer ID
N	1	$(0, 1)$	2
E	1	$(1, 2)$	1
S	1	$(2, 1)$	1

per Table 9 is 1. So, we have $T_1(\mu) = 1$. The corresponding trajectory for both pursuers, along with the UGS statuses (green or red with delay) encountered by them, are shown in Figs. 15–17. Here, the "red" observations made by the pursuers are color coded as per the pursuer's color. □

Theorem 9.4. $T_D(\mu) = D$, $D \geq 1$ *and* μ *is an optimal policy.*

Proof. We shall prove the result via mathematical induction.

Basic step. The result holds for $D = 1$, since $T_1(\mu) = 1$ from Lemma 9.3.

Induction step. Assume that for some $D \geq 2$,

$$T_M(\mu) = M, \quad M = 1, \ldots, (D-1). \tag{31}$$

We proceed to show that $T_D(\mu) = D$.

Recall that $\mathcal{C}_D$ is the initial condition, where the first pursuer is at location $(r+1, c+1)$ and observes delay, $D > 1$ and the second pursuer is at location (r, c) — see Fig. 14.

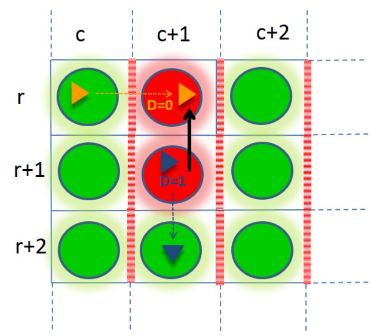

Fig. 15. Cellular network with two pursuers, and $D = 1$, and Intruder Strategy N

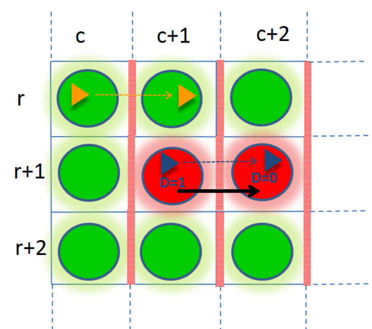

Fig. 16. Cellular network with two pursuers, and $D = 1$, and Intruder Strategy E.

January 5, 2022 1:48:12pm WSPC/284-US 2250005 ISSN: 2301-3850 2nd Reading

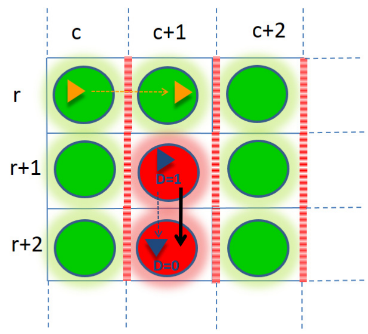

Fig. 17. Cellular network with two pursuers, and $D = 1$, and Intruder Strategy S.

To illustrate the result, we shall consider a few example intruder strategies and show that capture occurs in no more than D steps, when pursuit policy μ is employed.

(1) Suppose the intruder follows the sequence of actions: $E * W_{D-1}$, i.e. it goes east first, followed by any allowed sequence of actions indicated by W_{D-1}. In this case, under policy μ, both pursuers move east first and so, the first pursuer will observe delay $D-1$ and the second pursuer will observe a green UGS. But this situation is identical to $\mathcal{C}_{D-1}$. So, using the induction hypothesis, we have the worst-case steps to capture given by (refer Fig. 18),

$$1 + T_\mu(D-1) = 1 + (D-1) = D.$$

(2) Assume intruder goes towards S^D. First move of $P2$ is E and $P1$ is S. $P1$ will observe delay $D-1$ and $P2$ will observe a green UGS. As intruder moves towards "South", laser fence in "East" direction is not triggered, $P1$ will capture the intruder in D time steps, going further $D-1$ steps towards "South". $P2$, after encountering green UGS in its first move, changes its direction of move towards "South" (refer Fig. 19).

(3) Suppose the intruder follows the sequence of actions: $S^i E * W_{D-i-1}$, for some $i = 1, 2, \ldots, D-1$. As per policy μ, $P1$ will move i steps towards "South" and $P2$ will move $i-1$ steps towards "South" after making its first move towards "East". When in $(i+1)$th step, intruder makes an "East" turn, the information is known to $P1$ as laser fence is triggered, when it reaches there in ith step. Therefore, in $(i+1)$th step, $P1$ moves "East" and $P2$ moves "South". Delay observed by $P1$ is $D-i-1$. This situation is identical to $\mathcal{C}_{D-i-1}$. Again, using the induction hypothesis, we have the worst-case steps to capture given by (refer Fig. 20),

$$i + 1 + T_\mu(D-i-1) = i + 1 + (D-i-1) = D.$$

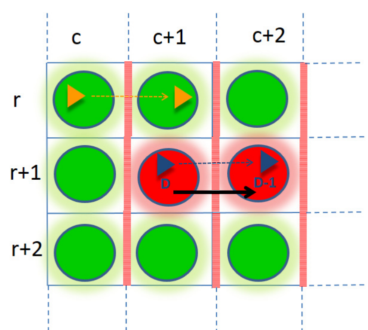

Fig. 18. Cellular network with two pursuers, and delay D, and Intruder Strategy $E * W_{D-1}$.

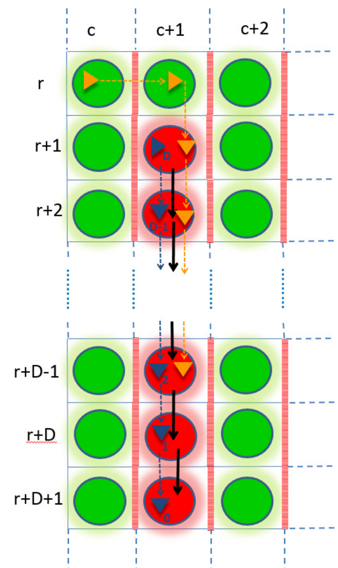

Fig. 19. Cellular network with two pursuers, and delay D, and Intruder Strategy S^D.

(4) Similarly, when intruder follows the sequence of actions: either N^D or $N^i E * W_{D-i-1}$, as per policy μ, the logic will be interchanged between $P1$ and $P2$ and "North" and "South", due to the symmetry of the graph.

(a) Assume intruder goes towards N^D. First move of $P2$ is E and $P1$ is S. $P2$ will observe delay $D-1$ and $P1$ will observe a green UGS. As intruder moves towards "North", laser fence in "East" direction is not triggered, $P2$ will capture the intruder in D time steps, going towards $D-1$ steps towards "North". $P1$, after encountering green UGS in its first move, changes its direction of move towards "North".

(b) Suppose the intruder follows the sequence of actions: $N^i E * W_{D-i-1}$, for some $i = 1, 2, \ldots, D-1$. As per policy μ, $P2$ will move $i-1$ steps towards "North" after making its first move towards "East" and $P1$ will move $i-1$ steps towards "North" after making its first move towards "South". When in $(i+1)$th step, intruder makes an "East" turn, the information is known to $P2$

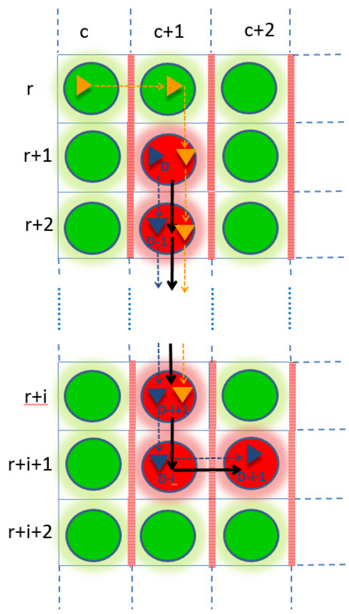

Fig. 20. Cellular network with two pursuers, and delay D, and Intruder Strategy $S^i E * W_{D-i-1}$.

as laser fence is triggered, when it reaches there in ith step. Therefore, in $(i+1)$th step, $P2$ moves "East" and $P1$ moves "North". Delay observed by $P2$ is $D-i-1$. This situation is identical to $\mathcal{C}_{D-i-1}$, "North" and "South" being symmetric. Again, using the induction hypothesis, we have the worst-case steps to capture given by

$$i+1+T_{\mu}(D-i-1) = i+1+(D-i-1) = D.$$

Therefore, it is shown that regardless of the intruder's strategy, the pursuers while employing μ will capture the intruder in no more than D steps. Indeed, Table 10 enumerates all possible intruder strategies and the corresponding steps to capture (and by whom) under policy μ.

It is clear that the intruder can do no better than D steps and so, $T_D(\mu) = D$. Since the optimal policy can do no worse than the policy μ, we have

$$T(D) \leq D, \quad \forall\, D > 0. \tag{32}$$

Table 10. Number of steps to capture the intruder for different intruder strategies.

Intruder strategy	Steps to capture	Pursuer ID
$E * W_{D-1}$	D	1 or 2
S^D	D	1
$S^i E * W_{D-i-1}$	D	1 or 2
N^D	D	2
$N^i E * W_{D-i-1}$	D	1 or 2

We shall now proceed to show that μ is a optimal pursuit policy. In order to prove the optimality of μ, it suffices to show that $T(D) \geq D, \forall D > 0$. The basic idea behind the construction of the lower bound is the following:

- If one were to restrict the set of trajectories of the intruder in (9.2) by requiring $w(2k) \in \hat{\mathcal{W}}(e(2k)) \subset \mathcal{W}(e(2k))$, one gets a lower bound for $T(D)$. Essentially, this is tantamount to optimizing the pursuer's policy over a restricted set of intruder trajectories.
- Let us restrict intruder's move only towards "East". As per explanation in Lemma 7.7, pursuer 1 should move towards "East". Because of speed advantage, in one move pursuer 1 at best reduces delay by 1. So in D steps, pursuer 1 will capture intruder. Hence, $T(D) \geq D$, $\forall\, D > 0$. Therefore, $T_D = D = T_D(\mu)$ and μ is an optimal policy. □

As already explained, with delay D, lowest possible capture time is D. So, three or more UVs will not improve performance achieved by two cooperative UVs.

10. Conclusion

A smart border management system consisting of UGSs and LFS as smart ground sensors and UVs as ground or airborne element has been proposed for intruder engagement. The terrain has been modeled as cellular structure consisting of rows and columns, equipped with the ground sensors. The main idea of modeling the terrain as cellular structure is because of practical significance. Functional model of UGS, LFS and pursuer–intruder dynamics have been described. Optimal solutions to minimum time capture problem have been obtained for three-row cases with a single pursuer. Because of additional information from laser fencing system, the optimal minimum time capture time has been improved significantly than employing only UGS for this case. In addition, the main contribution is on deriving optimal solutions to minimum time capture problem for four-row cases. Also an optimal cooperative pursuit policy for any number of rows has been derived for a two pursuer scenario, which also shows significant improvement over the corresponding UGS only configuration. Thus, the proposed smart border management system is applicable to engage intruders in a vast cross border scenario.

References

[1] J. G. Mooney, S. Haviland and E. N. Johnson, Collaborative autonomy for mapping, search, and pursuit, *Unmanned Syst.* **04**(02) (2016) 167–184.

[2] M. Ray, O. Evans and J. Jamieson, Three-dimensional laser radar for perimeter security, in *Electro-Optical Remote Sensing*, eds. G. W.

January 5, 2022 1:48:18pm WSPC/284-US 2250005 ISSN: 2301-3850 2nd Reading

Kamerman and D. V. Willetts, Vol. 5988 (International Society for Optics and Photonics, SPIE, 2005), pp. 49–60.

[3] C. Olsen, K. Kalyanam, W. Baker and D. Kunz, Maximal distance discounted and weighted revisit period: A utility approach to persistent unmanned surveillance, *Unmanned Syst.* **7**(4) (2019) 215–232.

[4] S. Semnani and O. Basir, Multi-target engagement in complex mobile surveillance sensor networks, *Unmanned Syst.* **5**(1) (2017) 31–43.

[5] M. Darrah, J. Wilhelm, T. Munasinghe, K. Duling, S. Yokum, E. Sorton, J. Rojas and M. Wathen, A flexible genetic algorithm system for multi-UAV surveillance: Algorithm and flight testing, *Unmanned Syst.* **3**(1) (2015) 49–62.

[6] J. Wilhelm, J. Rojas, G. Eberhart and M. Perhinschi, Heterogeneous aerial platform adaptive mission planning using genetic algorithms, *Unmanned Syst.* **05**(01) (2017) 19–30.

[7] H. Witsenhausen, A minimax control problem for sampled linear systems, *IEEE Trans. Autom. Control* **13** (1968) 5–21.

[8] D. P. Bertsekas and I. B. Rhodes, On the minimax reachability of target sets and target tubes, *Automatica* **7** (1971) 233–247.

[9] D. P. Bertsekas, Control of uncertain systems with a set-membership description of the uncertainty, Ph.D. thesis, Massachusetts Institute of Technology (1971).

[10] D. P. Bertsekas and I. B. Rhodes, Sufficiently informative functions and the minimax feedback control of uncertain dynamic systems, *IEEE Trans. Autom. Control* **18** (1973) 117–124.

[11] R. Isaacs, *Differential Games: A Mathematical Theory with Applications to Welfare and Pursuit, Control and Optimization* (John Wiley & Sons, 1965).

[12] G. T. Dzyubenko and B. N. Pshenichnyi, Discrete differential games with information lag, *Cybern. Syst. Anal.* **8**(6) (1972) 947–952.

[13] F. V. Fomin and D. M. Thilikos, An annotated bibliography on guaranteed graph searching, *Theor. Comput. Sci.* **399** (2008) 236–245.

[14] K. Krishnamoorthy, D. W. Casbeer, P. Chandler, M. Pachter and S. Darbha, UAV search & capture of a moving ground target under delayed information, in *51st IEEE Conf. Decision and Control (CDC)*, Maui, HI, 2012, pp. 3092–3097.

[15] K. Krishnamoorthy, S. Darbha, P. Khargonekar, D. W. Casbeer, P. Chandler and M. Pachter, Optimal minimax pursuit evasion on a Manhattan grid, in *American Control Conf.*, Washington, DC, 2013, pp. 3427–3434.

[16] K. Krishnamoorthy, S. Darbha, P. Khargonekar, P. Chandler and M. Pachter, Optimal cooperative pursuit on a Manhattan grid, in *AIAA Guidance, Navigation and Control Conf. (AIAA 2013-4633)*, Boston, MA, 2013, pp. 1–10.

[17] T. Parsons, Pursuit-evasion in a graph, *Theory and Applications of Graphs*, Lecture Notes in Mathematics, Vol. 8, No. 1 (Springer, Berlin, 1978), pp. 426–441.

[18] N. E. Clarke, A witness version of the cops and robber game, *Discrete Math.* **309**(10) (2009) 3292–3298.

Sufal Chandra Swar received his Bachelor of Engineering (B.E.) degree in Metallurgy from Bengal Engineering College (Deemed University) [at present, Indian Institute of Engineering, Science & Technology (IIEST)], Shibpur and Master of Technology (M.Tech.) degree in Computational Science from Indian Institute of Science (IISc), Bengaluru. He is a Scientist in Aeronautical Development Establishment (ADE), Defence R&D Organization (DRDO), Bengaluru. His areas of work include applied statistics, quality and reliability engineering, autonomous/cooperative mission control algorithms for unmanned vehicles.

Suresh Manickam obtained his Bachelor's degree in Electronics and Instrumentation Engineering from Annamalai University, Chidambaram and the Master's and Ph.D. in Aerospace Engineering from the Indian Institute of Science, Bengaluru. He is a scientist at the Aeronautical Development Establishment, Defence R&D Organization, Bengaluru, India. His areas of research interest are in flight mechanics, navigation, guidance, flight and mission control of aerospace vehicles.

David Casbeer is the team lead for the UAV Cooperative and Intelligent Control Team within the Control Science Center of Excellence in the Air Force Research Laboratory's Aerospace Systems Directorate. The UAV team focuses on decision making, planning and coordination for multiple autonomous UAVs acting and reacting in uncertain and adversarial environments. This team was awarded the AFOSR Star Team award for 2018–2020 for excellence in basic research. Dr. Casbeer received the B.S. and Ph.D. degrees from Brigham Young University in 2003 and 2009, respectively, where he advanced theory describing the statistics of decentralized estimation techniques. In 2016, Dr. Casbeer was awarded AFRL's Early Career Award for distinguished foundational research in multi-agent control. He serves as a Senior Editor for the *Journal of Intelligent and Robotic Systems* and an editor for the *AIAA Journal of Aerospace Information Systems*.

Krishna Kalyanam received the B.Tech. degree from the Indian Institute of Technology, Madras, India, in 2000, and the M. S. and Ph.D. degrees from the University of California at Los Angeles, CA, USA, in 2003 and 2005, respectively, all in Mechanical Engineering. After graduation, he worked as a Research Engineer with GE Global Research, Bengaluru, India. From 2009–2018, he was an on-site contractor/research scientist with the Autonomous Controls Branch, U.S. Air Force Research Laboratory, Dayton, OH, USA. From 2018–2021, he was a Sr. Scientist with the System Sciences Lab at the Palo Alto Research Center (Xerox PARC). He is currently an Aerospace Engineer with the Aviation Systems Division at the NASA Ames Research Center, Moffett Field, CA, USA. His current research interests include autonomous systems, stochastic optimization, human machine collaboration and cooperative control of unmanned air vehicles.

Swaroop Darbha received his B.Tech. degree from the Indian Institute of Technology at Madras in 1989, M.S. and Ph.D. degrees from the University of California at Berkeley in 1992 and 1994, respectively. Subsequently, he was a Visiting Post-doctoral Researcher at the California PATH program of the Institute for Transportation Studies at UC Berkeley till 1996. He joined Texas A&M University in January 1997 as an Assistant Professor, where he is currently the Gulf Oil/Thomas A. Dietz Professor. He is a fellow of ASME and SAE. He is interested in the areas of unmanned vehicles, intelligent transportation systems, control and estimation theory and optimization.